HEAT TRANSFER IN DUCTS OF VARYING CROSS-SECTION USING A LINEAR k-ε MODEL AND A PARABOLIC SOLVER

Edimilson J. Braga – e-mail: braga@mec.ita.br
Marcelo J.S. de-Lemos – e-mail: delemos@mec.ita.br
Departamento de Energia - IEME, Instituto Tecnológico de Aeronáutica - ITA
12228-900 São José dos Campos - SP - Brasil

Abstract. Heated turbulent confined jet flow is numerically investigated. The development of subsonic jets with higher and lower central velocity and temperature is considered. A marching-forward numerical integration technique is used to sweep the computational domain. Both cases of gradual enlargements or contractions of sinusoidal duct walls are calculated. Turbulence is handled with the standard linear isotropic k-ε model. Previous comparisons reproduced experimental data showing that, within contractions, turbulence is damped whereas, in diffusers, the valued of k is increased. Solution of the energy equation further shows interesting dissimilarities between turbulent kinetic energy and heat transfer. In contracting ducts, while turbulence in damped, the turbulent Nusselt number increases. Along enlargements, overall turbulent heat transfer is damped.

Keywords: Turbulent heat transfer, Coaxial jets, Diffusers and contractions

1. INTRODUCTION

Duct contractions or enlargements are found in a number of engineering equipment. Turbulent non-isothermal coaxial jets within such ducts can be encountered in industrial piping, jet-pumps, gas turbines and in air conditioning ducts, for example. Accurate determination of flow mixing and heat transfer rates in such devices contributes to efficiency increase, optimal design parameters and, ultimately, reduction of cost-benefit relationship.

Experimental work published on turbulent coaxial jets deals, in its majority, with sudden expansion flow into a stagnant surrounding (Buresti et al, 1998) or within a confining duct (Park & Chen, 1989). Measurements in two-phase systems (Albagli & Levy, 1991, Fan et al, 1996a) and computational studies applying Large Eddy Simulation to coaxial jets are also found in the literature (Knut & Moin, 1996). In all of the above, recirculating flow due to abrupt expansion precludes the use of the mathematical treatment below, which, in contrast, is based on a marching-forward technique (Patankar, 1988). The work of (Yule & Damou, 1992), presented results for confined coaxial turbulent jets with velocity ratio U_1/U_2 up to 30, being U_1 the central jet velocity. Both streams flowed into a convergent-divergent channel. Report was limited to mean axial velocity and axial turbulent intensity. Yet, their overall duct length was of a relative short size ($x/D = 4$).

Following this path, the work of (Matsumoto & de Lemos, 1990), presented results for the developing *time-averaged* and *turbulent* fields in a coaxial jet along a circular duct of constant area. Later, (de Lemos & Milan, 1997), extended their calculations to flow in long ducts through varying cross sections. In de Lemos & Braga, 1998, it was further considered coaxial jets with *higher* ($U_e > U_i$) and *lower* ($U_e < U_i$) annular velocity in *diverging* ($H>0$) and *converging* ($H<0$) ducts of the shape shown in Fig. 1. Similar results for ducts with plane walls have also been documented (de Lemos & Braga, 1999). Validation of the numerical values obtained has been achieved by comparisons with experiments (de Lemos & Braga, 2000a).

Heat transfer analysis followed with the work of de Lemos & Braga, 1999, who reported Nusselt numbers and turbulent kinetic energy in planar diffusers and contractions. Therein, flow and heat transfer properties of coaxial jets, with higher inner velocity ($U_i > U_e$) and temperature ($T_i > T_e$), were predicted. That work made use of the standard k-ε model, wall log-laws for velocity and temperature and the assumption of constant turbulent Prandtl number. Later, the sinusoidal geometry was investigated (de Lemos & Braga, 2000b) considering the case of $U_i < U_e$ and $T_i < T_e$. Interesting dissimilarity between heat transport and turbulence was calculated and a compilation and extension of the heat transfer analysis in such ducts has been presented (Braga & de Lemos, 2000). While turbulence was damped along accelerating flows (contractions), heat transfer was increased by a fair amount. This opposing behavior between turbulence and turbulent heat transfer is herein further investigated.

The present contribution extends the early heat transfer analysis and compiles computations for jets with higher and lower central velocity and temperature. Previously found dissimilarities between heat transfer and turbulence levels in plane wall ducts are computed for sinusoidal passages shown in Fig. 1.
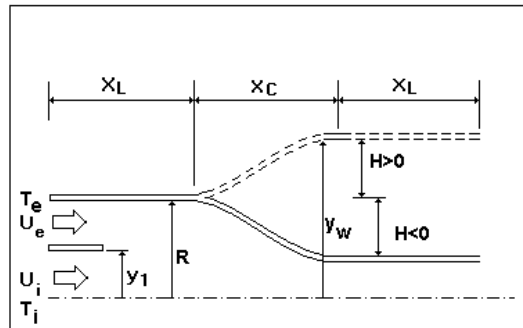

Figure 1 - Notation for general ducts with diverging (*H*>0) and converging (*H*<0) walls of sinusoidal shape.

2. MATHEMATICAL MODEL AND NUMERICS

2.1 Mean flow

The equations of continuity of mass, *x*-momentum and energy for a two-dimensional, source-free, low speed, planar/axi-symmetric turbulent mixing layer can be written as,

$$\frac{\partial\,(\,y^{\eta}\rho u\,)}{\partial x} + \frac{\partial(\,y^{\eta}\rho v\,)}{\partial y} = 0 \tag{1}$$

$$\rho u \frac{\partial u}{\partial x} + \rho v \frac{\partial u}{\partial y} = - \frac{\partial P}{\partial x} + \frac{1}{y^\eta} \frac{\partial}{\partial y} \left[y^\eta \ \mu_{eff} \frac{\partial u}{\partial y} \right] \qquad (2)$$

$$\rho u \frac{\partial T}{\partial x} + \rho v \frac{\partial T}{\partial y} = \frac{1}{y^\eta} \frac{\partial}{\partial y} \left[y^\eta \ \Gamma_{eff}^T \frac{\partial T}{\partial y} \right] \qquad (3)$$

In Eq. (1), Eq. (2) and Eq. (3) u, v are the velocity components in the axial and transverse direction, respectively, T is the temperature, ρ the fluid density, P the static pressure, and μ_{eff}, Γ_{eff}^T the coefficients of turbulent exchange given as $\mu_{eff} = \mu_t + \mu$ and $\Gamma_{eff}^T = \mu_t/\sigma_T + \mu/\mathrm{Pr}$, respectively. Also, μ is the molecular viscosity, Pr the fluid Prandtl number and μ_t and σ_T the turbulent viscosity and the Prandtl/Schmidt number, respectively. As usual, equations Eq. (1), Eq. (2) and Eq. (3) are written in a compact notation embracing planar (η=0) and axi-symmetric (η=1) cases.

2.2 Turbulence model

The turbulence model k-ε of Jones and Launder, 1972, has been used in the literature in a number of publications. In this approach, the turbulent viscosity mentioned above is calculated as $\mu_t = \rho c_\mu k^2/\varepsilon$ where c_μ is a constant. Here, as done in (de Lemos & Braga, 2000b), only the case involving flow regions of high local Reynolds numbers are considered (Launder and Spalding, 1974). With this, transport equations for k and ε can be written as,

$$\rho u \frac{\partial \phi}{\partial x} + \rho v \frac{\partial \phi}{\partial y} = \frac{1}{y^\eta} \frac{\partial}{\partial y} \left[y^\eta \ \Gamma_\phi \frac{\partial \phi}{\partial y} \right] + S_\phi \qquad (4)$$

In Eq. (4) ϕ stands for k or ε. The diffusion coefficients are given by $\Gamma_{eff}^k = \mu + \mu_t/\sigma_k$ and $\Gamma_{eff}^\varepsilon = \mu + \mu_t/\sigma_\varepsilon$ where the σ's are the turbulent Prandtl/Schmidt numbers for k and ε, respectively. The last terms in Eq. (4) are known as "source" terms and are given by $S_k = \rho\,(P_k - \varepsilon)$ and $S_\varepsilon = \rho\frac{\varepsilon}{k}(c_1 P_k - c_2 \varepsilon)$, being c_1=1.47, c_2=1.92 and c_μ=0.09. The production term reads $P_k = \mu_t/\rho\,(\partial U/\partial y)^2$.

2.3 Boundary conditions and Computational Details.

The numerical approach adopted here and in (de Lemos & Braga, 2000b), is the parabolic solver technique of Patankar & Spalding, 1972, and Patankar, 1988. For clarity, it is reviewed below.

Inlet flow is given a uniform distribution. For temperature, constant value of T prevails over the inlet. Also, the values of k and ε at entrance were given by $k_{in} = 10^{-3} U_m$ and $\varepsilon_{in} = k_{in}^{3/2}/Ky'$ where U_m is the overall mean velocity, K is the von Kármán constant (K=0.4) and y' the distance to the wall. For the centerline (y=0) the symmetry condition is implemented for all dependent variables ϕ=U, T, k and ε as $\partial \phi/\partial y)_{y=0} = 0$. Wall proximity is handled with the **Wall Function** approach (Launder & Spalding, 1974) giving for the wall shear stress,

$$\tau_w = \left(U_N\, \rho\, c_\mu^{\frac{1}{4}}\, k_N^{\frac{1}{2}}\right) \bigg/ \frac{1}{K} \ln\left[E\, y_N\, \frac{\rho\, (c_\mu^{\frac{1}{2}} k_N)^{\frac{1}{2}}}{\mu}\right] \qquad (5)$$

where *E* a constant. In Eq. (5) the subscript "*N*" identifies the grid point closest to the wall. In that region, the use of the **Wall Function** associated with the assumption of "<u>local equilibrium</u>" for turbulence ($P_k=\varepsilon$) gives $k_N = \tau_w / (\rho\, c_\mu)^{\frac{1}{2}}$ *and* $\varepsilon_N = k_N^{3/2}/K\, y_N$. Rewriting Eq. (5) in the form $\tau_w = \lambda\mu(\partial U/\partial y)$ gives further,

$$\lambda = \begin{cases} 1 \quad \text{for laminar flow} \\[2mm] \dfrac{K\, y_N\, \dfrac{\rho\, (c_\mu^{\frac{1}{2}} k_N)^{\frac{1}{2}}}{\mu}}{\ln\left[E\, y_N\, \dfrac{\rho\, (c_\mu^{\frac{1}{2}} k_N)^{\frac{1}{2}}}{\mu}\right]} \quad \text{for turbulent flow} \end{cases} \qquad (6)$$

For temperature, the **Wall Law** is given by,

$$T^+ = (T_N - T_w)\rho c_p\, c_\mu^{\frac{1}{4}} k_N^{\frac{1}{2}} \big/ q_w = \frac{Pr_t}{K} \ln\left[E\, y_N\, \frac{\mu(c_\mu^{\frac{1}{2}} k_N)^{\frac{1}{2}}}{\rho}\right] + 12.5\, Pr^{\frac{2}{3}} + 2.12\, Pr - c_q \qquad (7)$$

where the last term in Eq. (**7**) fits experimental data and has been proposed by (Kader & Yaglom, 1972). It reads $c_q = 5.3$ for Pr<0.5 and $c_q = 1.5$ for Pr≥0.5. Either case, constant T_w or constant q_w, is analyzed with Eq. (**7**). The wall heat flux can be further given after rearranging Eq. (**7**) in the form $q_w = -\lambda_T\, \dfrac{\mu c_p}{Pr}\, \dfrac{\partial T}{\partial y}$ where;

$$\lambda_T = \begin{cases} 1 \quad \text{for laminar flow} \\[2mm] \dfrac{K\, y_N\, \dfrac{\rho\, (c_\mu^{\frac{1}{2}} k_N)^{\frac{1}{2}}}{\mu}\, Pr}{\left(\sigma_T \ln\left[E\, y_N\, \dfrac{\rho\, (c_\mu^{\frac{1}{2}} k_N)^{\frac{1}{2}}}{\mu}\right] + c_q^* K\right)} \quad \text{for turbulent flow} \end{cases} \qquad (8)$$

with $c_q^* = 12.5\, Pr^{\frac{2}{3}} + 2.12\, Pr - c_q$.

Determination of the unknown pressure gradient is handled as explained in (Patankar, 1988). That approach consists in finding the zero of a function representing the discrepancy, at the downstream position, between the *calculated* and *real* duct area. All transport equations for the mean and turbulent fields were solved by means of the marching-forward method of (Patankar, 1988).

2.4 Code Validation

The compilation work of (Spencer et al, 1995), seems to be the only available experimental data bank for turbulent flow within contractions and diffusers. Therein, experimental data from 11 institutions around the world, taken for flow of air and water in contraction and diffuser, were compared with each other and with computational results using commercial CFD codes. Experimentally observed turbulence damping in contractions and corresponding enhancement in diffusers, reported in detail by (Spencer et al, 1995), was

correctly simulated in de Lemos & Braga, 2000a. In that paper, direct comparisons with experimental data have shown that for contractions up to 21° and for diffusers up to 5°, the model and numerical scheme employed reproduced the basic features of the flow. Beyond those values, as expected, deterioration of the prediction quality was observed since parabolic equations were considered. The computer code developed was then fully checked and results validated (de Lemos & Braga, 2000a).
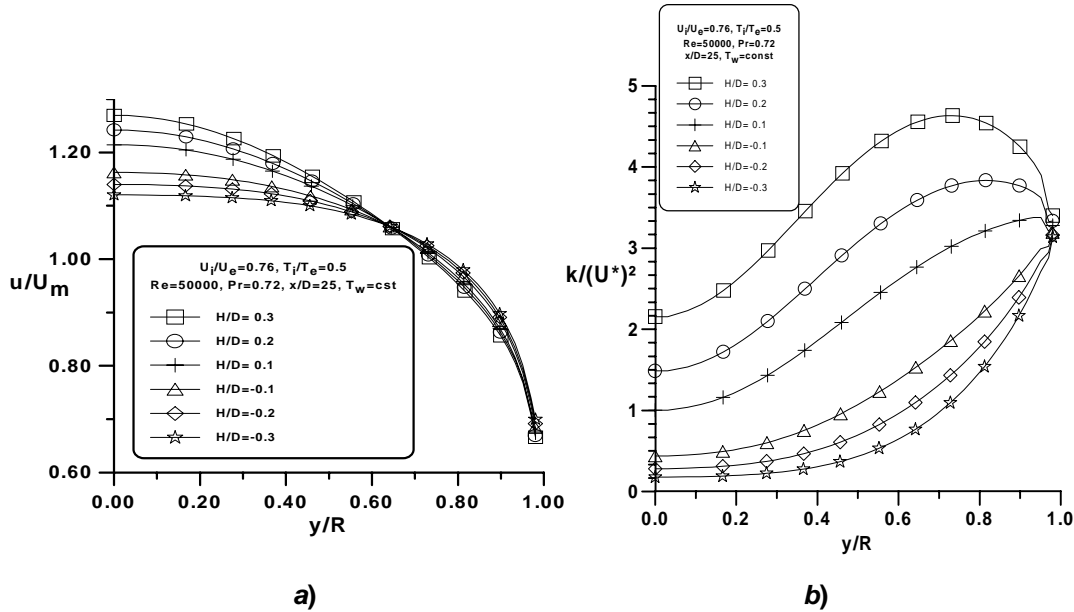

a)   b)

Figure 2 - Profiles at short duct exit: *a*) velocity, *b*) turbulent kinetic energy.

3. RESULTS AND DISCUSSION

3.1 Jets with lower central velocity and temperature

Calculations were then performed in a 25 diameters long diverging/converging section preceded and followed by a length equal to $x/D=5$ (see Fig. 1). An internal jet with velocity 30% lower than the concentric external stream ($U_i=0.76U_e$) was considered with its temperature being half the outer jet temperature ($T_i=0.5T_e$). This situation would be typical of equipment designed to exchange heat by mixing two streams of different temperatures.

Mean velocity and k profiles at the duct exit are presented in Fig. 2 for different values of H/D. The six curves shown for converging/diverging ducts with constant T_w would be the same if they were calculated with q_w=constant. Both boundary conditions are condensed into only one data set since b.c. type for temperature is immaterial when calculating flow based on constant property hypothesis. Figure 2 indicates that converging passages flatten velocity profiles at a faster rate than enlargement sections.

Figure 3 show results for the temperature profiles for the cases of q_w=constant and T_w=constant at the downstream position x/D=25. One can see that a flatter temperature distribution is observed along the diverging sections. When these results are compared to the ones in Fig. 2*b*, **dissimilarity** between turbulence and Nusselt number is anticipated. Nusselt number behavior for long ducts with varying cross section has been presented in de Lemos & Braga, 1999, and de Lemos & Braga, 2000b. For the flow considered herein (heated jet flow in short ducts), results for Nusselt will be presented later. For now, it is sufficient to note that

converging sections will quickly mix streams of different velocity (flatter u/U_m in Fig. 2) but will fail to do the same when temperature is of concern (steeper curves in Fig. 3).
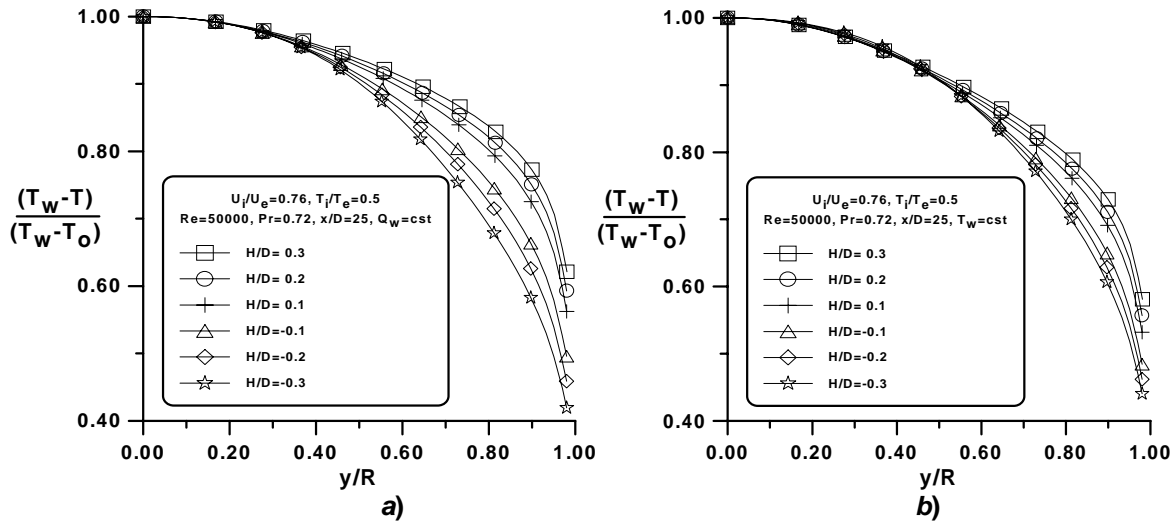

Figure 3 - Temperature profiles at short duct exit: *a)* q_w = constant and T_w = constant.

3.2 Jets with higher central velocity and temperature

An internal jet with velocity 30% higher than the concentric external stream ($U_i=1.3U_e$) was also considered, being its temperature twice the one of the outer jet ($T_i=2.0T_e$).

Mean velocity profiles at the duct exit are presented in Fig. 4. As in the case of Fig. 2, the four curves shown for constant T_w and q_w in Fig. 4 are condensed in only two data sets. This is because the boundary condition for temperature does not affect the flow when calculations are based on the constant property hypothesis. Nevertheless, both curve sets are shown in the figure for clarity and consistency of all numerical results herein. Fig. 4 again indicates that converging passages flatten velocity profiles at a faster rate than enlargement sections.

During profile development the steep temperature gradient in the inlet is, at the end, smoothed out and the flow becomes quite mixed. This indicates that this mixing is stronger when mean flow decelerates, leading to flatter temperature profiles at the duct exit. This idea is better understood in Figure 5 where results for the temperature profiles at the downstream position x/D=25 are compiled. One can see that a flatter temperature distribution is observed along the diverging section. When these results are compared to the ones in Figure 4, here also **dissimilarity** between heat and turbulent kinetic energy is apparent. When the central jet is of higher velocity and temperature, flattening of temperature profiles seems to be even stronger.

3.2 Nusselt number

The Nusselt number for both boundary conditions for temperature, for different jet configurations and for expanding or contracting ducts, are compiled in Fig. 6. The figure compares results with the case of constant area duct. Independently of the initial jet configuration, and as seen on previous figures (Fig. 3), contracting ducts decrease turbulent heat transfer through the wall. The opposing trend is observed for expanding passages. In addition, when the internal jet is hotter and flows faster, overall Nu is greater. This last effect is in coherence with Fig. 7 which shows a better mixing of the two streams for $U_i>U_e$, and

$T_i > T_e$. When designing heat transfer equipment, engineers may take the results herein as an aid in analyzing mixing in channels.

Before concluding this work the authors would like to justify their use of the word "***dissimilarity***" when describing the opposing behavior for *Nu* and *k*. Usually these two flow properties are expected to be similar. In a duct of constant area, higher levels of *k* imply in higher turbulent transport of momentum across the flow. This, in turn, is associated with a higher skin friction factor. Heat transport follows the same trend. If the cross sectional are is varied, however, results herein indicate a different behavior. Accelerating the flow in a contracting duct will also increase wall shear stress and *Nu,* but this process is not related to generation of additional turbulence. In this sense, the word dissimilarity is here made use of.
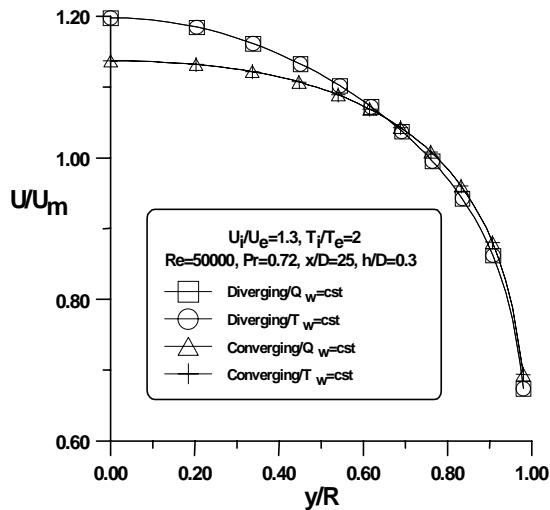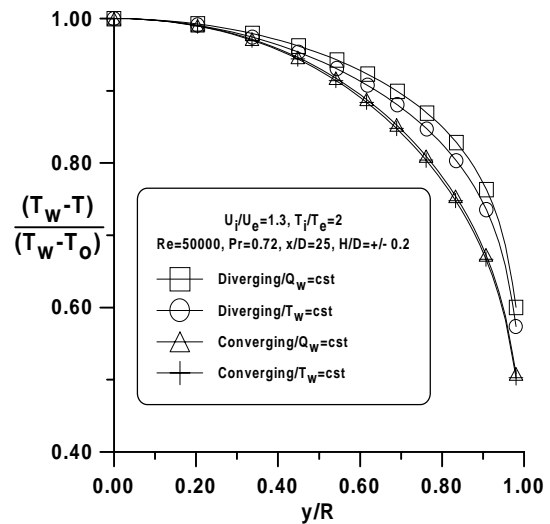

Figure 4 - Velocity profiles at short duct exit.

Figure 5 – Temperature profiles at short duct exit.

4. CONCLUDING REMARKS

This paper presented computations with the standard k-ε model for simulation of confined non-isothermal jet flow in ducts of varying cross-section. Diverging and converging ducts were calculated showing different or *dissimilar* behavior for turbulence and Nusselt number. In general, accelerated flows in a convergent duct reduce turbulence level although *Nu* increases by a fairly amount. The opposing trend is observed in expanding passages (decelerating flow). Also in short ducts, and for the conditions here analyzed, flattening of the velocity profile in converging sections is accompanied by bulging of non-dimensional values for temperature. Therefore, in both configurations studied, dissimilarities between heat and momentum transfer become apparent. The results herein are expected to contribute to the design and analysis of engineering equipment involving concentric turbulent jets. Potential application of this study may include heat exchanger design and analysis.
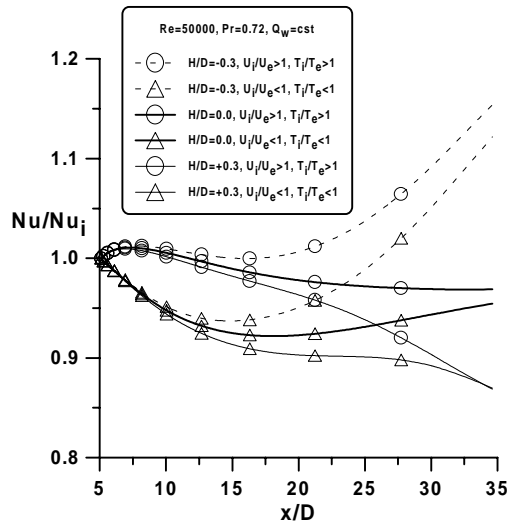
Figure 6 - Nusselt number for contracting, straight and expanding ducts
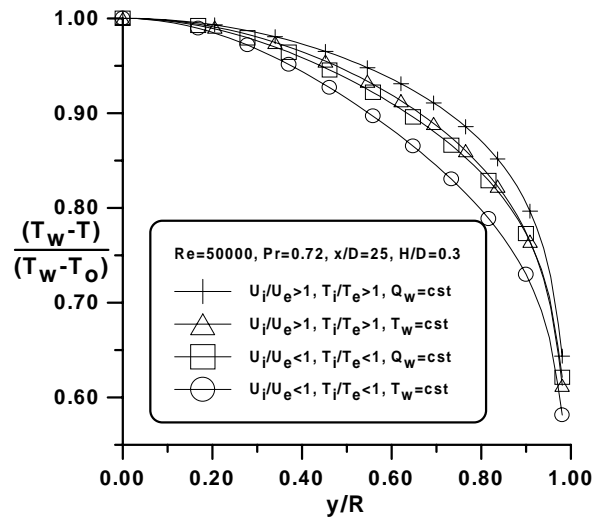

Figure 7 -Effect of inlet temperature and velocity ratios on temperature profiles, H/D=0.3.

REFERENCES

Albagli, D., Levy, Y., 1991, Experimental Study on Confined Two-Phase Jets, *Journal of Thermophysics and Heat Transfer*, v. 5. n. 3, pp. 387-393.

Braga, E.J., de Lemos, M.J.S., 1999, Numerical Analysis of Coaxial Turbulent Jets in Diffusers and Contractions (on CDROM), *Proc. of COBEM99 - 15th Braz. Congr. Mech. Eng.*, ISBN: 85-85769-03-3, November 22-26, Águas de Lindóia, São Paulo, Brazil.

Braga, E.J., de Lemos, M.J.S., 2000, Dissimilarities Between Nusselt Number Andturbulent Kinetic Energy for Flow in Ducts of Varying Cross-Sectional Area, *accepted for presentation at* CONEM2000*, National Mechanical Engineering Congress*, August 7-11, Natal, Rio Grande do Norte, Brazil.

Buresti, G., Petagna, P., Talamelli, A., 1998, Experimental Investigation on The Turbulent Near-Field of Coaxial Jets, *Experimental Thermal and Fluid Science*, v 17, n. 1-2, pp. 18-26.

de Lemos, M.J.S., Braga, E.J., 1998, Numerical Investigation of Turbulent Duct Flow Through Gradual Enlargements and Contractions, ASME-FED-vol.245, ISBN: 0-7918-1950-7, *Proc. of FEDSM-Fluid Eng. Div. Summer Meeting*, Washington, D.C., USA, June 21-25.

de Lemos, M.J.S., Braga, E.J., 1999, Characteristics of Turbulent Heat Transfer in Coaxial Jets Through Gradual Enlargements and Contractions, **Paper NHTC-0165**, *33rd National Heat Transfer Conference*, Albuquerque, New Mexico, USA, August 15-17.

de Lemos, M.J.S., Braga, E.J., 2000a, Simulation of Turbulent Flow in Contracting and Expanding Ducts With a Linear k-ε Model, **Paper FEDSM2000-11083**, *2000 ASME Fluids Engineering Summer Conference*, Boston, Massachusetts, USA, June 11-15.

de Lemos M.J.S., Braga, E.J., 2000b, Turbulent Heat Transfer in Confined Coaxial Jets Through Ducts of Gradually Varying Cross Section, *Turbulent Heat Transfer*, **Paper NHTC2000-12089,** *34th National Heat Transfer Conference*, August 20-22, 2000, Pittsburgh, Pennsylvania, USA.

de Lemos, M.J.S., Milan, A., 1997, Mixing of Confined Coaxial Turbulent Jets in Ducts of Varying Cross Section, *CD-ROM of COBEM97 – 12th. Braz. Cong. Mech Eng.*, Bauru, São Paulo, Brazil, December 8-12.

Fan, J.; Zhao, H., Cen, K., 1996a, Two-Phase Velocity Measurements in Particle-Laden Coaxial Jets, *Chemical Engineering Journal*, v. 63, n. 1, p. 11-17.

Jones, W.P., Launder, B.E., 1972, The Prediction of Laminarization With a Two-Equation Model of Turbulence, *Int. J. Heat & Mass Transfer*, vol. 15, pp. 301-314.

Kader, B.A., Yaglom, A.M., 1972, Heat and Mass Transfer Laws for Fully Turbulent Wall Flows, *Int. J. Heat & Mass Transf.,* vol. 15, pp. 2329-2351.

Knut, A, Moin, P., 1996, Large-Eddy Simulation of Turbulent Confined Coannular Jets, *Journal of Fluid Mechanics,* vol. 315, p. 387-411.

Launder, B.E., Spalding, D.B., 1974, The Numerical Computation of Turbulent Flows, *Comp. Math. App. Mech. Eng.*, vol. 3, pp. 269-289.

Matsumoto, E., 1990a, Estudo de Jatos Confinados, *MSc Thesis*, ITA/CTA.

Matsumoto, E., de Lemos, M.J.S., 1990, Development of an Axi-Symmetric Mixing Layer in a Duct of Constant Cross Section, *Proc. of 3rd Braz. Therm. Sci. Meet.*, vol. I, pp. 381-385, Itapema, Brazil, December 10-12.

Park, C.J.; Chen, L.D., 1989, Experimental Investigation of Confined Turbulent Jets. Part I. Single-Phase Data, *AIAA Journal*, v. 27, n. 11, pp. 1506-1510.

Patankar, S.V., 1988, PARABOLIC SYSTEMS, Chapter 2 of Handbook of Numerical Heat Transfer, Rohsenow ed., John Wiley & Sons, New York.

Patankar, S.V., Spalding, D.B., 1972, A Calculation Procedure for Heat, Mass and Momentum Transfer in Three-Dimensional Parabolic Flows, *Int. J. Heat & Mass Transf.,* vol. 15, pp. 1787-1806.

Spencer, E.A., Heitor, M.V., Castro, I.P., 1995, Intercomparison of Measurements and Computations of Flow Through a Contraction and a Diffuser, *Flow Measurement and Instrumentation,* v. 6, n. 1, p. 3-14.

Yule, A.J., Damou, M., 1992, Axisymmetrical Turbulent Jet Flows in a Duct of Varying Area, *Experim. Thermal and Fluid Science,* v. 5, n. 4, p. 499-505.